ACS NANO
Cite This: ACS Nano 2018, 12, 6777−6783
www.acsnano.org

ARTICLE

An Ultrasensitive Diagnostic Biochip Based on Biomimetic Periodic Nanostructure-Assisted Rolling Circle Amplification

Qian Yao,[†,§] Yingqian Wang,[†,§] Jie Wang,[†] Shaomin Chen,[‡] Haoyang Liu,[†] Zhuoran Jiang,[†] Xiaoe Zhang,[†] Songmei Liu,[‡] Quan Yuan,*[,†] and Xiang Zhou*[,†]

[†]College of Chemistry and Molecular Sciences, Key Laboratory of Biomedical Polymers of Ministry of Education, Key Laboratory of Analytical Chemistry for Biology and Medicine (Ministry of Education), Wuhan University, Wuhan 430072, China

[‡]Center for Gene Diagnosis, Zhongnan Hospital of Wuhan University, Wuhan University, Wuhan 430072, China

Supporting Information

ABSTRACT: Developing portable and sensitive devices for point of care detection of low abundance bioactive molecules is highly valuable in early diagnosis of disease. Herein, an ultrasensitive photonic crystals-assisted rolling circle amplification (PCs-RCA) biochip was constructed and further applied to circulating microRNAs (miRNAs) detection in serum. The biochip integrated the optical signal enhancement capability of biomimetic PCs surface with the thousand-fold signal amplification feature of RCA. The biomimetic PCs displayed periodic dielectric nanostructure and significantly enhanced the signal intensity of RCA reaction, leading to efficient improvement of detection sensitivity. A limit of detection (LOD) as low as 0.7 aM was obtained on the PCs-RCA biochip, and the LOD was 7 orders of magnitude lower than that of standard RCA. Moreover, the PCs-RCA biochip could discriminate a single base variation in miRNAs. Accurate quantification of ultralow-abundance circulating miRNAs in clinical serum samples was further achieved with the PCs-RCA biochip, and patients with the nonsmall cell lung carcinoma were successfully distinguished from healthy donors. The PCs-RCA biochip can detect bioactive molecules with ultrahigh sensitivity and good specificity, making it valuable in clinical disease diagnosis and health assessment.

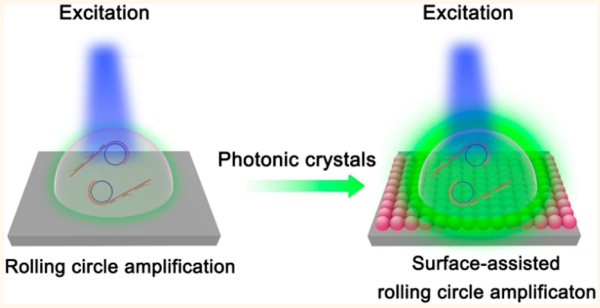

KEYWORDS: *biochip, photonic crystals, rolling circle amplification, circulating miRNA, cancer*

Early diagnosis of disease can significantly reduce mortality and improve survival rates.[1] Bioactive molecules including nucleic acids, proteins, sugars, and small metabolites play crucial roles in the early diagnosis of disease.[2−4] MicroRNAs (miRNAs) act as post-transcription regulators of gene expression and participate in various biological processes such as cell growth, proliferation, and apoptosis.[5,6] Increasing evidence suggests that the dysregulated expression of serum circulating miRNAs is highly correlated with certain human diseases, including various types of cancer.[4,7−11] Thus, serum circulating miRNAs are identified as noninvasive biomarkers,[12] and great efforts have been made to develop methods for highly sensitive detection for circulating miRNAs. Rolling circle amplification (RCA) is an isothermal and enzymatic process that holds great potential in the detection of DNA, RNA, and protein in genomics and proteomics.[13,14] Due to the enzymatic process of RCA, thousand-fold signal amplification can be achieved.[15−17] Moreover, RCA is suitable for point-of-care detection of targets since it only involves isothermal reaction.[18−20] In spite of such virtue, RCA still faces formidable challenges in the detection of serum circulating miRNAs. The limit of detection (LOD) of standard RCA is only femtomolar, and it cannot detect the trace circulating miRNAs in clinical serum samples.[15,21,22] Developing a strategy to improve the sensitivity of RCA for direct serum miRNA detection is highly valuable in early diagnosis of disease.

Nature has created a great variety of structural color materials that can precisely confine, control, and manipulate light by their regularly photonic nanostructures.[23] For instance, the wings of the Morpho butterfly usually exhibit bright colors due to the Bragg diffraction effect generated by the periodic ordered structures of wings.[23−26] Inspired by the natural creatures, many artificial photonic materials with controllable structures and light-manipulating functions have been developed.[23] Photonic crystals (PCs) are one of the most

Received: March 14, 2018
Accepted: June 20, 2018
Published: June 20, 2018

DOI: 10.1021/acsnano.8b01950
ACS Nano 2018, 12, 6777−6783

Scheme 1. Schematic Illustration of the miRNA-Responsive PCs-RCA Biochip

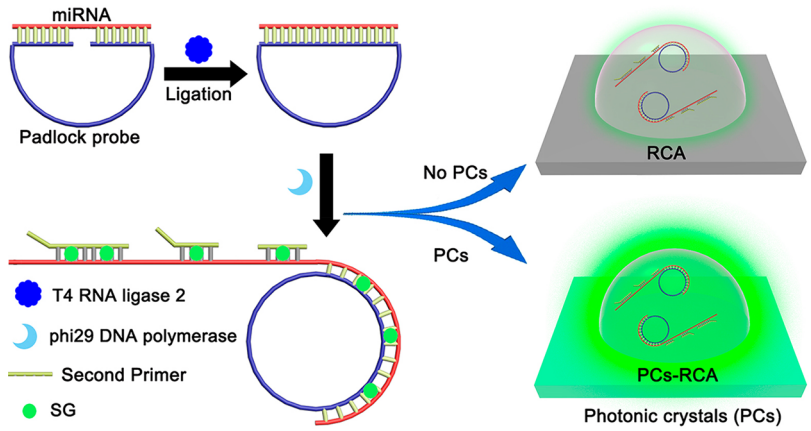

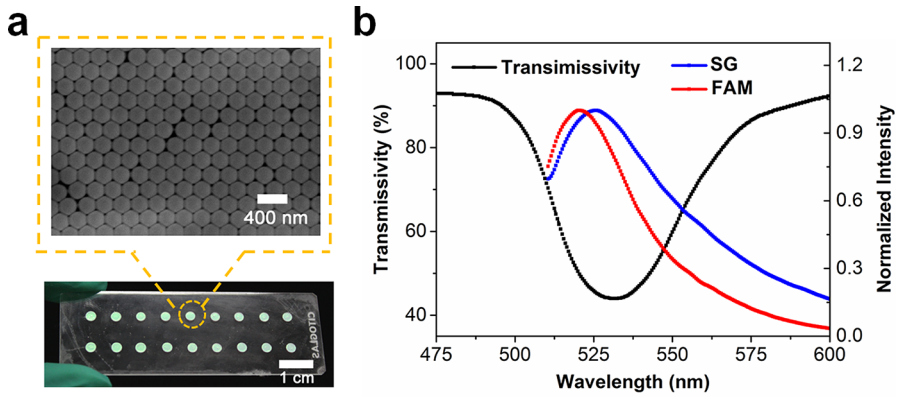

Figure 1. (a) Photograph of the prepared PCs in sunlight. Insert: SEM image of the periodic nanostructure of PCs. (b) Transmittance spectrum of the designed PCs and fluorescence spectra of SG and FAM.

widely studied artificial periodic nanostructures that display special ability to enhance the intensity of optical species.[27] Generally, when the emission light of fluorophores on PCs surface overlaps with the photonic band gap of the PCs, the emission light is unable to pass through the PCs and will be effectively reflected in the direction of the band gap.[23] The reflected light signal can be simultaneously collected with the emission signal of fluorophores, thus leading to the enhancement of signal intensity.[28] In the past years, PCs have been largely used to enhance the signal intensity in biosensing and hundred-fold enhancement of sensitivity has been achieved.[29−34] Therefore, PCs can serve as an ideal platform to improve the detection sensitivity of RCA by enhancing the signal intensity.

The schematic representation of PCs-assisted RCA (PCs-RCA) biochip is illustrated in Scheme 1. Target miRNA acts as the template to ligate the padlock probe and further initiate the RCA reaction to produce long double-stranded DNA (dsDNA). SYBR Green I (SG) molecules specifically bind to the minor groove of dsDNA to produce fluorescence signal.[35] Due to the overlap between the photonic band gaps of PCs and the emission band of SG, the fluorescence intensity of SG-dsDNA on the PCs surface can be significantly enhanced, thus leading to improvement of the detection sensitivity of RCA. This PCs-RCA biochip rationally combines the prominent fluorescence enhancement capability of PCs with the signal amplification feature of RCA, making it possible for detection of miRNAs with low expression levels in serum samples.

RESULTS AND DISCUSSION

The PCs were fabricated by depositing hydrophilic polystyrene (PS) spheres (Figures S1 and S2) onto hydrophobic polydimethylsiloxane (PDMS) substrate. Figure 1a and Figure S3 show that PS spheres self-assembled into a closely packed periodic nanostructure on PDMS after evaporation. Bright green color is observed on the PCs when it is exposed to sunlight, suggesting that green light can be efficiently reflected by the PCs surface. The capability of the prepared PCs for enhancing the fluorescence intensity of green fluorophores such as SG or carboxyfluorescein (FAM) was further investigated. Figure 1b shows that the photonic band gap of PCs covers from 500 to 570 nm, consistent with the above phenomenon that the PCs surface can selectively reflect green light. The emission bands of SG and FAM well overlap the photonic band gap of PCs, making the PCs surface ideal to reflect the fluorescence signal of such green fluorophores.

The solution of FAM-labeled DNA (FAM-DNA) was further employed to test the signal enhancement capability of the PCs surface, as illustrated in Figure 2a. The photographs of FAM-DNA solution on bare PDMS and on PCs surface under ultraviolet light excitation were provided (Figure 2b). The FAM-DNA solution on bare PDMS displays negligible green fluorescence, whereas bright green fluorescence is clearly observed from FAM-DNA solution on PCs surface, clearly showing that the biomimetic periodic nanostructure of PCs surface can efficiently enhance the fluorescence intensity of FAM-DNA. Quantitative characterization about the capability

DOI: 10.1021/acsnano.8b01950
ACS Nano 2018, 12, 6777−6783

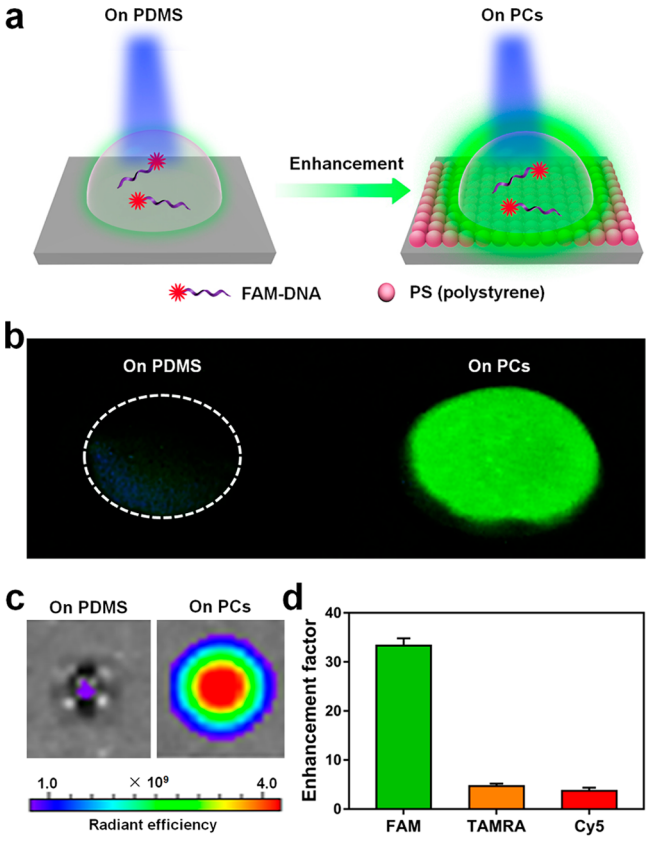

Figure 2. (a) Schematic illustration of FAM-DNA solution on PDMS and on PCs surface under excitation. (b) The photographs of FAM-DNA solution on bare PDMS and on PCs surface under excitation with a portable UV lamp. (c) Fluorescence images of FAM-DNA on PDMS and on PCs surface captured with a PE Spectrum and Quantum FX imaging system. (d) The enhancement factors of the PCs surface for FAM, TAMRA, and Cy5, respectively.

of the PCs surface in signal enhancement was further conducted with a PE Spectrum and Quantum FX imaging system. As shown in Figure 2c, FAM-DNA solution deposited on the PCs is much brighter than that on bare PDMS substrate, which can be attributed to the efficient reflection of the green fluorescence from FAM-DNA by the periodic dielectric nanostructures of PCs surface. Moreover, the signal intensity of FAM-DNA solution is measured to be enhanced by about 33-fold on PCs surface (Figure S4). The influence of the PCs surface on the fluorescence from other organic dyes including 5-carboxytetramethylrhodamine (TAMRA) and *N*,*N*′-(dipropyl)-tetramethyl-indodicarbocyanine (Cy5) was also investigated. As shown in Figure 2d, the PCs surface displays the highest enhancement factor to FAM fluorescence, which can be ascribed to the well overlap of FAM emission with the photonic band gap of PCs. These results clearly demonstrated that the designed PCs could significantly enhance signal intensity of green fluorophores by its uniform periodic dielectric nanostructure.

The capability of PCs to improve the sensitivity of RCA was further tested. Let-7a miRNA was employed as the target. The let-7a is one of the earliest found miRNA that has been confirmed to be dysregulated in several cancers.[36,37] Recent research suggests that serum let-7a miRNA can serve as biomarker for the diagnosis of nonsmall cell lung carcinoma (NSCLC).[38,39] Gel electrophoresis confirms that the let-7a miRNA successfully initiated the RCA reaction (Figures S5–S7). Due to the excellent signal enhancement capability of the PCs, RCA reaction on PCs surface shows much brighter fluorescence than standard RCA at the same concentration (Figure 3a). Moreover, when the concentration of miRNA is

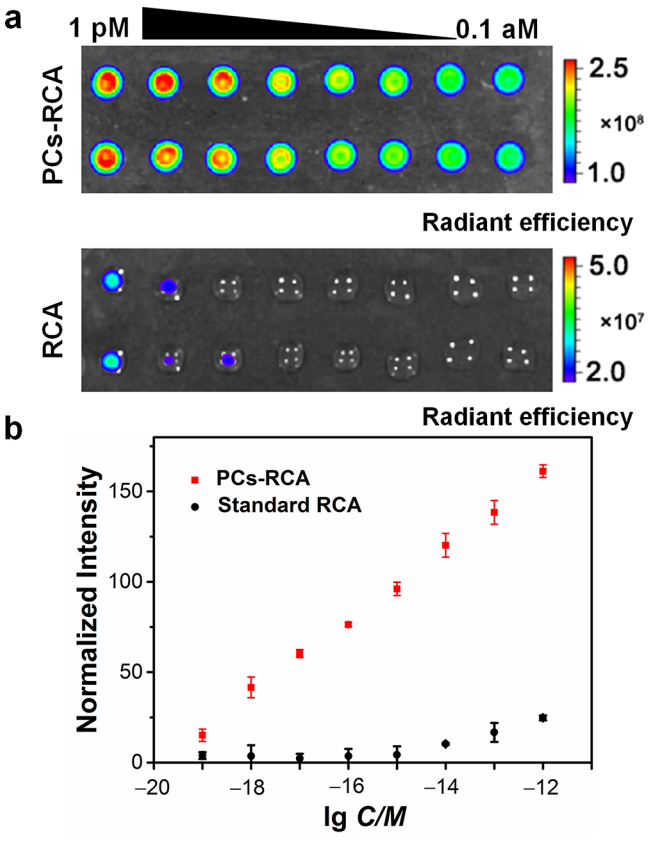

Figure 3. (a) Fluorescent images of let-7a miRNA-initiated RCA reactions at different let-7a concentrations on PCs surface (upper panel) and on bare PDMS (lower panel). (b) The relationship between the fluorescence intensity and the concentration of let-7a miRNA. Error bars show the standard deviation of three replicate measurements.

lower than 10 fM, the signal from the standard RCA cannot be detected. The same result can be observed when the fluorescence intensity of standard RCA products is measured by fluorescence spectrum (Figure S8). Also, as for let-7a miRNA detected on PCs dots without RCA process, the signal of let-7a miRNA solution could not be recognized when the concentration of let-7a miRNA was lower than 10 fM (Figure S9). In contrast, the RCA reaction on PCs surface shows strong fluorescence even with the let-7a miRNA concentration as low as 0.1 aM, clearly showing that the designed PCs can drastically enhance the signal of RCA to improve the detection sensitivity. The LOD of standard RCA is determined to be 10 fM. Whereas, the PCs-RCA biochip shows a LOD of 0.7 aM (Figure 3b), nearly 5 orders of magnitude lower than that of standard RCA. Such a low LOD corresponds to approximately 8 copies of let-7a miRNA molecules in a sample volume of 20 μL, clearly showing the high sensitivity of the PCs-RCA biochip in detecting let-7a miRNA. The regression equation of PCs-RCA biochip in let-7a miRNA detection is $F = 20.5 \times \lg C/M + 403.5$ with a correlation coefficient $R^2 = 0.9976$.

DOI: 10.1021/acsnano.8b01950
ACS Nano 2018, 12, 6777–6783

Moreover, a wide liner range from 0.1 aM to 1 pM is obtained with the PCs-RCA biochip in let-7a miRNA detection. The above results thus clearly show that ultrahigh sensitivity can be achieved by integrating the optical signal enhancement function of PCs and the signal amplification capability of RCA.

The specificity of the PCs-RCA biochip was further investigated. Since the let-7a miRNA shows high sequence homology to other let-7 family members, high specificity is required in the detection of serum circulating miRNA.[40,41] The response of the PCs-RCA biochip in the presence of let-7a, let-7c, let-7f, miR-21, miR-122, miR-155, and miR-199 was systematically examined (Figure 4). Among these miRNAs, let-7a, let-7c, and let-7f have their sequences differ by only one base at different sites. As shown in Figure S10, the PCs dots added with let-7a miRNA display much higher fluorescence intensity than those added with other miRNAs including let-7c and let-7f miRNA, suggesting that the PCs-RCA biochip can effectively distinguish miRNAs even with a single base difference. The signal intensity produced by let-7a miRNA is approximately 3.5-fold higher than that produced by let-7c miRNA and 7-fold higher than that produced by let-7f miRNA. These results demonstrate the high specificity of the PCs-RCA biochip, showing its good promise in serum circulating miRNA detection.

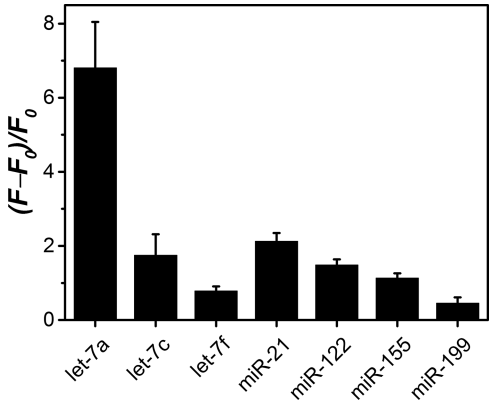

Figure 4. $(F - F_0)/F_0$ value of the PCs-RCA biochip in response to let-7a, let-7c, let-7f, miR-21, miR-122, miR-155, and miR-199 miRNAs at the concentration of 1 nM. F_0 and F are the fluorescence intensity in the absence and presence of miRNA, respectively. Error bars show the standard deviation of three replicate measurements.

The performance of the PCs-RCA biochip in the detection of let-7a miRNA in serum samples was further tested. Fetal bovine serum (FBS) spiked with synthetic let-7a miRNA at different concentrations was employed as the standard solutions. The response of the PCs-RCA biochip to the standard solutions was systematically measured. As shown in Figure 5a and 5b, a good linear relationship between the signal intensity of PCs dots and let-7a miRNA concentration is obtained in 7 orders of magnitude from 1 aM to 1 pM. The regression equation is $F = 25.9 \times \lg C/M + 484.16$ with a correlation coefficient $R^2 = 0.9915$. These results suggest that the biosensing performance of the PCs-RCA biochip was not significantly affected by background compounds in serum. The concentration of let-7a miRNA in serum samples from 48 donors, 24 healthy donors and 24 NSCLC patients, was further analyzed with the PCs-RCA biochip according to the above calibration curve. As shown in Figure 5c, serum samples from NSCLC patients produce much weaker signal intensity than that from healthy donors, indicating the down-regulated expression of let-7a miRNA in NSCLC patients. The quantification results in Figure 5d further show that the average expression level of let-7a miRNA in serum samples from healthy donor is about 2 times of that in serum samples from NSCLC patients, in good agreement with previous reports.[42] The above results thus clearly demonstrate the good promise of the PCs-RCA biochip in direct analysis of low abundance bioactive molecules in clinical samples, which can provide valuable information for health assessment and early diagnosis of disease.

To further confirm the reliability of PCs-RCA biochip in analyzing clinical samples, the concentration of let-7a miRNA in serum samples was in parallel measured with RT-qPCR. As shown in Figure 6, RT-qPCR measurements also indicate the down-regulated expression of let-7a miRNA in NSCLC patients, consistent with the results provided by PCs-RCA biochip. Moreover, the results obtained by PCs-RCA biochip on both healthy donors and NSCLC patients are close to those obtained by RT-qPCR. The t test further confirms that the quantification results provided by the PCs-RCA biochip do not differ significantly from those obtained by RT-qPCR ($p > 0.05$). The above results thus clearly demonstrate that the developed PCs-RCA biochip is highly reliable for serum circulating miRNA detection, suggesting its good promise in the analysis of low-abundance bioactive molecules in clinical samples.

CONCLUSIONS

We have developed an ultrasensitive biochip by designing PCs-assisted RCA reaction to achieve massive signal amplification for serum miRNA detection. The PCs-RCA biochip allows for sensitive detection of target miRNA with a LOD as low as 0.7 aM and a wide liner range of 8 orders of magnitude. Moreover, the PCs-RCA biochip possesses excellent specificity, and it can discriminate miRNAs with a single base difference. Due to its ultrahigh sensitivity and excellent specificity, trace target miRNA in serum samples from NSCLC patients was accurately quantified by the PCs-RCA biochip. The developed PCs-RCA biochip holds great potential in ultrasensitive detection of bioactive molecules, and it can further contribute to areas such as disease diagnosis and health assessment.

MATERIALS AND METHODS

Materials and Reagents. The sequences of all DNA and RNA oligonucleotides are provided in Table S1. DNAs were purchased from Sangon (Shanghai, China), and RNAs were purchased from Takara Biotechnology (Dalian, China). All of the oligonucleotides were purified by high-performance liquid chromatograph (HPLC). T4 RNA ligase 2 and phi29 DNA polymerase were purchased from New England Biolab (Beijing, China). SYBR green I (SG), dNTP (10 mM), and ribonuclease inhibitor were purchased from Thermo Scientific (USA). Polydimethylsiloxane (PDMS, Sylgard 184 silicone elastomer kit, Dow), curing agent, monodispersed latex spheres polystyrene (PS, m/v = 10%) were obtained from Dow Corning (USA).

MiRNA-Initiated RCA Reaction. First, 10 μL of mixed solution containing phosphorylated linear DNA template (0.2 pmol), miRNA with certain concentration (from 10 pM to 0.1 aM), 1 μL of 10 × T4 RNA ligase 2 buffer, and 40 U of ribonuclease inhibitor was prepared. The solution was heated to 65 °C and kept at this temperature for 5 min. The solution was further cooled to 25 °C and kept for 40 min. Then, T4 RNA ligase 2 (2 U) was added into the above solution, and

DOI: 10.1021/acsnano.8b01950
ACS Nano 2018, 12, 6777–6783

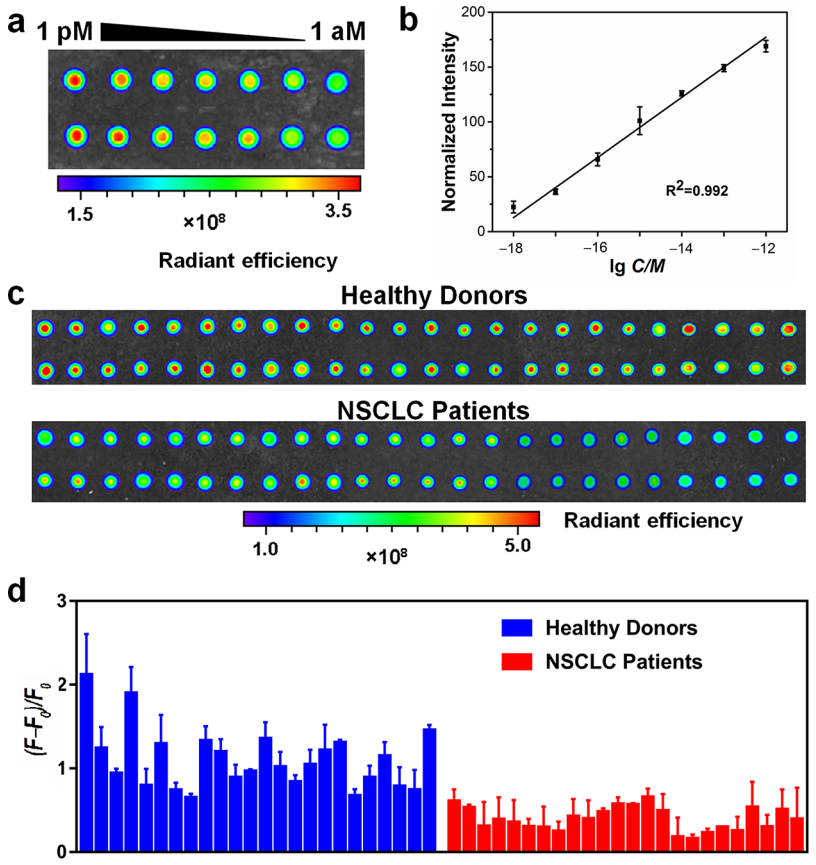

Figure 5. (a) Fluorescence image of the PCs-RCA biochip with the addition of standard let-7a miRNA-FBS solution. (b) The linear correlation between the fluorescent intensity and the concentration of let-7a miRNA. (c) Fluorescence image of the PCs-RCA biochip with the addition of serum samples from healthy donors and NSCLC patients. (d) The $(F - F_0)/F_0$ value of the PCs-RCA biochip in response to the serum samples, where F and F_0 were the fluorescence intensity in the presence of serum sample and the average value of the healthy donors, respectively. Error bars show the standard deviation of three replicate measurements.

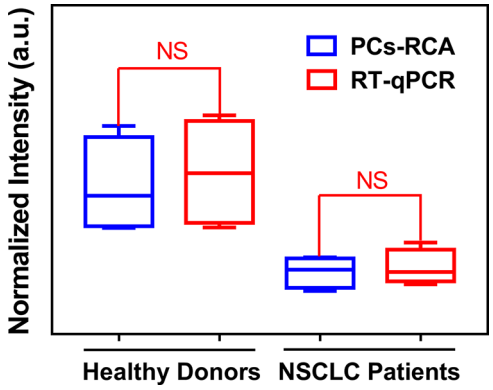

Figure 6. Comparing the let-7a miRNA quantification results provided by the PCs-RCA biochip and RT-qPCR. The *t* test was performed with $p = 0.05$. NS = not significant. Error bars show the standard deviation of three replicate measurements.

the resultant mixture was incubated at 39 °C for 1.5 h and was further denatured at 75 °C for 10 min. For exonuclease experiment, 1 μL of 10 × Exo I buffer and 0.5 μL of Exo I were added into the above solution to remove any remained linear DNA. The solution was heated to 37 °C and kept at this temperature for 30 min, followed by enzyme deactivation at 85 °C for 10 min. The ligated DNA templates were analyzed by 12% native polyacrylamide gel electrophoresis (120 V, 60 min). The ligation product was further added into 10 μL of RCA reaction mixture containing 2 μM of second primer (SP), 1 mM of dNTP, 2 μL of 10 × phi29 DNA polymerase buffer, 1 μL of 1 mg/mL BSA, and 20 U of phi29 DNA polymerase. The RCA reaction was performed at 30 °C for 2 h and further terminated by incubation at 65 °C for 10 min.

Fabrication of PCs Substrate. The PCs substrate was fabricated by solvent evaporation method. PDMS and curing agent (m/m = 1:1) were mixed and stirred adequately for 30 min. Then the mixture was treated under vacuum until no bubbles were observed. To fabricate PDMS-covered substrate, the above mixture was spin-coated on a glass slide followed by drying at 60 °C overnight. Next, 10 μL of the monodispersed carboxyl-modified polystyrene (PS) spheres (diluted with ultrapure water in a 1:4 v/v ratio) dropped vertically onto the PDMS substrate, and the substrate was kept at 40 °C until the PCs droplet was dried. The prepared PCs substrates were kept at a dry condition for further use.

Detection of let-7a miRNA with the PCs-RCA Biochip. For the detection of let-7a miRNA, 1 μL of 20 × SG was added to 20 μL of let-7a miRNA-initiated RCA products, and the resultant solution was incubated for 10 min at room temperature. Then 4 μL of the above products was dropped on the PCs dots, and the fluorescence pictures were captured by the PE Spectrum and Quantum FX imaging system.

Confirming the RCA Reaction with Electrophoresis. The RCA reaction was confirmed with a restriction enzyme digestion method reported previously.[43] A reaction solution containing digestion template (DT, 0.2 pmol), let-7a miRNA with different concentration, 1 μL of 10 × T4 RNA ligase 2 buffer, and 40 U of ribonuclease inhibitor was prepared. The reaction solution was treated at 65 °C for 5 min followed by cooling to 25 °C for 40 min. Then T4 RNA ligase 2 (2 U) was added in to the reaction solution. The mixture was incubated at 39 °C for 1.5 h and was denatured at 75 °C

DOI: 10.1021/acsnano.8b01950
ACS Nano 2018, 12, 6777−6783

for 10 min. Then the product of the ligation product was added to 10 μL of RCA reaction mixture containing 2 μM digestion second primer (DSP), 1 mM of dNTP, 2 μL of 10 × phi29 DNA polymerase buffer, 1 μL of 1 mg/mL BSA, and 20 U of phi29 DNA polymerase. The RCA reaction was performed at 30 °C for 24 h and terminated by incubation at 65 °C for 10 min. After that, 2 μL of 10 × cutsmart buffer and 0.5 μL of XhoI were added into the above solution. The reaction mixture was then incubated at 37 °C for 12 h and denatured at 65 °C for 20 min. The digestion procedure was designed to convert long RCA product into monomeric units (60 nt) to facilitate gel-based DNA concentration analysis. Then, 2.5 μL of 1 μM monomeric digestion product (MDP, 60 nt) and 2.5 μL of 1 μM reference DNA (RD, 70 nt) were added into 10 μL of the digestion product. The as prepared solution was then analyzed by 20% denature PAGE gel, and the gel was further stained with Gel Red before scanning. The concentration of the RCA product was calculated according to the fluorescence ratio between the monomeric digestion product band and the reference DNA band at each let-7a miRNA concentration.

Testing the Specificity of the PCs-RCA Biochip. The reaction was performed in 10 μL of ligation system containing padlock probe (0.2 pmol), 1 μL of 10 × T4 RNA ligase 2 buffer, 40 U of ribonuclease inhibitor, and 2 nM of each miRNAs (let-7a, let-7c, let-7f, miR-21, miR-122, miR-155, miR-199). The solution was heated to 65 °C and kept for 5 min. Then the solution was cooled to 25 °C and kept for 40 min. After that, T4 RNA ligase 2 (2 U) was added into the above solution, and the resultant mixture was incubated at 39 °C for 1.5 h, followed by denaturation at 75 °C for 10 min. Then the product of the ligation product was added to the 10 μL of RCA reaction mixture containing 2 μM SP, 1 mM dNTP, 2 μL of 10 × phi29 DNA polymerase buffer, 1 μL of 1 mg/mL BSA, and 20 U of phi29 DNA polymerase. The RCA reaction was performed at 30 °C for 2 h and further terminated by incubation at 65 °C for 10 min. Then 1 μL of 20 × SG was added to 20 μL of the each miRNA-initiated RCA product, and the solution was incubated for 10 min at room temperature. Then 4 μL of the each RCA products was dropped on the PCs dots, and the fluorescence images of the PCs dots were measured with a PE Spectrum and Quantum FX bioimaging system.

Quantification of let-7a miRNA in Serum Samples with PCs-RCA Biochip. The serum samples from 24 NSCLC patients and 24 healthy donors were provided by Zhongnan Hospital, Wuhan. Typically, 80 μL of 1 × PBS was added into to 20 μL of serum sample, and the solution was heated to 95 °C for 5 min. Then the solution was cooled rapidly to 4 °C and kept for 3 min.[44] Then the denatured serum lysates were centrifuged at 17,000 × *g* for 20 min at 4 °C. Finally, 2 μL of the supernatant was added to ligation and RCA reaction system. The reaction products treated with SG were further dropped on PCs dots, and the quantification was performed with the above-mentioned procedures.

ASSOCIATED CONTENT

Supporting Information

The Supporting Information is available free of charge on the ACS Publications website at DOI: 10.1021/acsnano.8b01950.

Oligonucleotide sequences used in this work, TEM image and size distribution of PS spheres, SEM images of the PCs, gel electrophoresis, let-7a miRNA detection on PCs without RCA, detection of let-7a miRNA in serum samples from healthy donors and NSCLC patients (PDF)

AUTHOR INFORMATION

Corresponding Authors

*E-mail: xzhou@whu.edu.cn.

*E-mail: yuanquan@whu.edu.cn.

ORCID

Jie Wang: 0000-0003-4170-8470

Songmei Liu: 0000-0001-9276-6078

Quan Yuan: 0000-0002-3085-431X

Xiang Zhou: 0000-0002-1829-9368

Author Contributions

§Q.Y. and Y.W. contributed equally to this work.

Notes

The authors declare no competing financial interest.

ACKNOWLEDGMENTS

This work was supported by the National Natural Science Foundation of China (21432008, 21721005, and 91753201).

REFERENCES

(1) Fu, J.; Wang, H. Precision Diagnosis and Treatment of Liver Cancer in China. *Cancer Lett.* **2018**, *412*, 283−288.

(2) Wu, L.; Qu, X. Cancer Biomarker Detection: Recent Achievements and Challenges. *Chem. Soc. Rev.* **2015**, *44*, 2963−2997.

(3) Sawyers, C. L. The Cancer Biomarker Problem. *Nature* **2008**, *452*, 548−552.

(4) Zen, K.; Zhang, C. Y. Circulating MicroRNAs: A Novel Class of Biomarkers to Diagnose and Monitor Human Cancers. *Med. Res. Rev.* **2012**, *32*, 326−348.

(5) Bartel, D. P. MicroRNAs: Target Recognition and Regulatory Functions. *Cell* **2009**, *136*, 215−233.

(6) Selbach, M.; Schwanhausser, B.; Thierfelder, N.; Fang, Z.; Khanin, R.; Rajewsky, N. Widespread Changes in Protein Synthesis Induced by MicroRNAs. *Nature* **2008**, *455*, 58−63.

(7) Chen, X.; Ba, Y.; Ma, L.; Cai, X.; Yin, Y.; Wang, K.; Guo, J.; Zhang, Y.; Chen, J.; Guo, X.; Li, Q.; Li, X.; Wang, W.; Zhang, Y.; Wang, J.; Jiang, X.; Xiang, Y.; Xu, C.; Zheng, P.; Zhang, J.; et al. Characterization of MicroRNAs in Serum: A Novel Class of Biomarkers for Diagnosis of Cancer and Other Diseases. *Cell Res.* **2008**, *18*, 997−1006.

(8) Shen, J.; Todd, N. W.; Zhang, H.; Yu, L.; Lingxiao, X.; Mei, Y.; Guarnera, M.; Liao, J.; Chou, A.; Lu, C. L.; Jiang, Z.; Fang, H.; Katz, R. L.; Jiang, F. Plasma MicroRNAs as Potential Biomarkers for Non−Small−Cell Lung Cancer. *Lab. Invest.* **2011**, *91*, 579−587.

(9) Cortez, M. A.; Bueso-Ramos, C.; Ferdin, J.; Lopez-Berestein, G.; Sood, A. K.; Calin, G. A. MicroRNAs in Body Fluids−The Mix of Hormones and Biomarkers. *Nat. Rev. Clin. Oncol.* **2011**, *8*, 467−477.

(10) Gong, X.; Zhou, W.; Chai, Y.; Yuan, R.; Xiang, Y. MicroRNA−Induced Cascaded and Catalytic Self−Assembly of DNA Nanostructures for Enzyme−Free and Sensitive Fluorescence Detection of MicroRNA from Tumor Cells. *Chem. Commun.* **2016**, *52*, 2501−2504.

(11) Yu, Y. Q.; Wang, J. P.; Zhao, M.; Hong, L. R.; Chai, Y. Q.; Yuan, R.; Zhuo, Y. Target−Catalyzed Hairpin Assembly and Intramolecular/Intermolecular Co−Reaction for Signal Amplified Electrochemiluminescent Detection of MicroRNA. *Biosens. Bioelectron.* **2016**, *77*, 442−450.

(12) Mitchell, P. S.; Parkin, R. K.; Kroh, E. M.; Fritz, B. R.; Wyman, S. K.; Pogosova-Agadjanyan, E. L.; Peterson, A.; Noteboom, J.; O'Briant, K. C.; Allen, A.; Lin, D. W.; Urban, N.; Drescher, C. W.; Knudsen, B. S.; Stirewalt, D. L.; Gentleman, R.; Vessella, R. L.; Nelson, P. S.; Martin, D. B.; Tewari, M. Circulating MicroRNAs as Stable Blood−Based Markers for Cancer Detection. *Proc. Natl. Acad. Sci. U. S. A.* **2008**, *105*, 10513−10518.

(13) Zhao, W.; Ali, M. M.; Brook, M. A.; Li, Y. Rolling Circle Amplification: Applications in Nanotechnology and Biodetection with Functional Nucleic Acids. *Angew. Chem., Int. Ed.* **2008**, *47*, 6330−6337.

(14) Ali, M. M.; Li, F.; Zhang, Z.; Zhang, K.; Kang, D. K.; Ankrum, J. A.; Le, X. C.; Zhao, W. Rolling Circle Amplification: A Versatile Tool for Chemical Biology, Materials Science and Medicine. *Chem. Soc. Rev.* **2014**, *43*, 3324−3341.

(15) Zhou, Y.; Huang, Q.; Gao, J.; Lu, J.; Shen, X.; Fan, C. A Dumbbell Probe−Mediated Rolling Circle Amplification Strategy for

DOI: 10.1021/acsnano.8b01950
ACS Nano 2018, 12, 6777−6783

Highly Sensitive MicroRNA Detection. *Nucleic Acids Res.* **2010**, *38*, e156.
(16) Zhao, Y.; Chen, F.; Li, Q.; Wang, L.; Fan, C. Isothermal Amplification of Nucleic Acids. *Chem. Rev.* **2015**, *115*, 12491−12545.
(17) Xu, Y.; Wang, H.; Luan, C.; Fu, F.; Chen, B.; Liu, H.; Zhao, Y. Porous Hydrogel Encapsulated Photonic Barcodes for Multiplex MicroRNA Quantification. *Adv. Funct. Mater.* **2018**, *28*, 1704458.
(18) Liu, M.; Hui, C. Y.; Zhang, Q.; Gu, J.; Kannan, B.; Jahanshahi-Anbuhi, S.; Filipe, C. D.; Brennan, J. D.; Li, Y. Target−Induced and Equipment−Free DNA Amplification with a Simple Paper Device. *Angew. Chem., Int. Ed.* **2016**, *55*, 2709−2713.
(19) Goo, N. I.; Kim, D. E. Rolling Circle Amplification as Isothermal Gene Amplification in Molecular Diagnostics. *BioChip J.* **2016**, *10*, 262−271.
(20) Chen, A.; Ma, S.; Zhuo, Y.; Chai, Y.; Yuan, R. In Situ Electrochemical Generation of Electrochemiluminescent Silver Naonoclusters on Target−Cycling Synchronized Rolling Circle Amplification Platform for MicroRNA Detection. *Anal. Chem.* **2016**, *88*, 3203−3210.
(21) Li, Y.; Liang, L.; Zhang, C. Y. Isothermally Sensitive Detection of Serum Circulating miRNAs for Lung Cancer Diagnosis. *Anal. Chem.* **2013**, *85*, 11174−11179.
(22) Ge, J.; Zhang, L. L.; Liu, S.-J.; Yu, R. Q.; Chu, X. A Highly Sensitive Target−Primed Rolling Circle Amplification (TPRCA) Method for Fluorescent *in Situ* Hybridization Detection of MicroRNA in Tumor Cells. *Anal. Chem.* **2014**, *86*, 1808−1815.
(23) Zhao, Y.; Xie, Z.; Gu, H.; Zhu, C.; Gu, Z. Bio−Inspired Variable Structural Color Materials. *Chem. Soc. Rev.* **2012**, *41*, 3297−3317.
(24) Potyrailo, R. A.; Starkey, T. A.; Vukusic, P.; Ghiradella, H.; Vasudev, M.; Bunning, T.; Naik, R. R.; Tang, Z.; Larsen, M.; Deng, T.; Zhong, S.; Palacios, M. A.; Grande, J. C.; Zorn, G.; Goddard, G.; Zalubovsky, S. Discovery of The Surface Polarity Gradient on Iridescent Morpho Butterfly Scales Reveals A Mechanism of Their Selective Vapor Response. *Proc. Natl. Acad. Sci. U. S. A.* **2013**, *110*, 15567−15572.
(25) Potyrailo, R. A.; Bonam, R. K.; Hartley, J. G.; Starkey, T. A.; Vukusic, P.; Vasudev, M.; Bunning, T.; Naik, R. R.; Tang, Z.; Palacios, M. A.; Larsen, M.; Le Tarte, L. A.; Grande, J. C.; Zhong, S.; Deng, T. Towards Outperforming Conventional Sensor Arrays with Fabricated Individual Photonic Vapour Sensors Inspired by Morpho Butterflies. *Nat. Commun.* **2015**, *6*, 7959.
(26) Chung, K.; Yu, S.; Heo, C. J.; Shim, J. W.; Yang, S. M.; Han, M. G.; Lee, H. S.; Jin, Y.; Lee, S. Y.; Park, N.; Shin, J. H. Flexible, Angle−Independent, Structural Color Reflectors Inspired by Morpho Butterfly Wings. *Adv. Mater.* **2012**, *24*, 2375−2379.
(27) Zhao, Y.; Zhao, X.; Gu, Z. Photonic Crystals in Bioassays. *Adv. Funct. Mater.* **2010**, *20*, 2970−2988.
(28) Fenzl, C.; Hirsch, T.; Wolfbeis, O. S. Photonic Crystals for Chemical Sensing and Biosensing. *Angew. Chem., Int. Ed.* **2014**, *53*, 3318−3335.
(29) Hou, J.; Zhang, H.; Yang, Q.; Li, M.; Song, Y.; Jiang, L. Bio−Inspired Photonic−Crystal Microchip for Fluorescent Ultratrace Detection. *Angew. Chem., Int. Ed.* **2014**, *53*, 5791−5795.
(30) Hou, J.; Zhang, H.; Yang, Q.; Li, M.; Jiang, L.; Song, Y. Hydrophilic−Hydrophobic Patterned Molecularly Imprinted Photonic Crystal Sensors for High−Sensitive Colorimetric Detection of Tetracycline. *Small* **2015**, *11*, 2738−2742.
(31) Qin, M.; Huang, Y.; Li, Y.; Su, M.; Chen, B.; Sun, H.; Yong, P.; Ye, C.; Li, F.; Song, Y. Rainbow Structural−Color Chip for Multisaccharide Recognition. *Angew. Chem., Int. Ed.* **2016**, *55*, 6911−6914.
(32) George, S.; Chaudhery, V.; Lu, M.; Takagi, M.; Amro, N.; Pokhriyal, A.; Tan, Y.; Ferreira, P.; Cunningham, B. T. Sensitive Detection of Protein and MiRNA Cancer Biomarkers Using Silicon−Based Photonic Crystals and A Resonance Coupling Laser Scanning Platform. *Lab Chip* **2013**, *13*, 4053−4064.
(33) Frascella, F.; Ricciardi, S.; Pasquardini, L.; Potrich, C.; Angelini, A.; Chiado, A.; Pederzolli, C.; De Leo, N.; Rivolo, P.; Pirri, C. F.; Descrovi, E. Enhanced Fluorescence Detection of MiRNA−16 on A Photonic Crystal. *Analyst* **2015**, *140*, 5459−5463.
(34) Pasquardini, L.; Potrich, C.; Vaghi, V.; Lunelli, L.; Frascella, F.; Descrovi, E.; Pirri, C. F.; Pederzolli, C. Smart Detection of MicroRNAs through Fluorescence Enhancement on A Photonic Crystal. *Talanta* **2016**, *150*, 699−704.
(35) Dave, N.; Chan, M.; Huang, P.; Smith, B. D.; Liu, J. Regenerable DNA−Functionalized Hydrogels for Ultrasensitive, Instrument−Free Mercury(II) Detection and Removal in Water. *J. Am. Chem. Soc.* **2010**, *132*, 12668−12673.
(36) Liu, K.; Zhang, C.; Li, T.; Ding, Y.; Tu, T.; Zhou, F.; Qi, W.; Chen, H.; Sun, X. Let-7a Inhibits Growth and Migration of Breast Cancer Cells by Targeting HMGA1. *Int. J. Oncol.* **2015**, *46*, 2526−2534.
(37) Seyyedi, S. S.; Soleimani, M.; Yaghmaie, M.; Ajami, M.; Ajami, M.; Pourbeyranvand, S.; Alimoghaddam, K.; Akrami, S. M. Deregulation of MiR−1, MiR486, and Let-7a in Cytogenetically Normal Acute Myeloid Leukemia: Association with NPM1 and FLT3 Mutation and Clinical Characteristics. *Tumor Biol.* **2016**, *37*, 4841−4847.
(38) Johnson, C. D.; Esquela-Kerscher, A.; Stefani, G.; Byrom, M.; Kelnar, K.; Ovcharenko, D.; Wilson, M.; Wang, X.; Shelton, J.; Shingara, J.; Chin, L.; Brown, D.; Slack, F. J. The let−7 MicroRNA Represses Cell Proliferation Pathways in Human Cells. *Cancer Res.* **2007**, *67*, 7713−7722.
(39) Takamizawa, J.; Konishi, H.; Yanagisawa, K.; Tomida, S.; Osada, H.; Endoh, H.; Harano, T.; Yatabe, Y.; Nagino, M.; Nimura, Y.; Mitsudomi, T.; Takahashi, T. Reduced Expression of the let−7 MicroRNAs in Human Lung Cancers in Association with Shortened Postoperative Survival. *Cancer Res.* **2004**, *64*, 3753−3756.
(40) Deng, R.; Tang, L.; Tian, Q.; Wang, Y.; Lin, L.; Li, J. Toehold−Initiated Rolling Circle Amplification for Visualizing Individual MicroRNAs *in Situ* in Single Cells. *Angew. Chem., Int. Ed.* **2014**, *53*, 2389−2393.
(41) Zhu, G.; Liang, L.; Zhang, C. Y. Quencher−Free Fluorescent Method for Homogeneously Sensitive Detection of MicroRNAs in Human Lung Tissues. *Anal. Chem.* **2014**, *86*, 11410−11416.
(42) Igaz, I.; Igaz, P. Tumor Surveillance by Circulating MicroRNAs: A Hypothesis. *Cell. Mol. Life Sci.* **2014**, *71*, 4081−4087.
(43) Liu, M.; Zhang, Q.; Chang, D.; Gu, J.; Brennan, J. D.; Li, Y. A DNAzyme Feedback Amplification Strategy for Biosensing. *Angew. Chem., Int. Ed.* **2017**, *56*, 6142−6146.
(44) Abe, K. Direct PCR from Serum. *Methods Mol. Biol.* **2003**, *226*, 161−166.

DOI: 10.1021/acsnano.8b01950
ACS Nano 2018, 12, 6777−6783